

000 001 002 003 004 005 006 007 008 009 010 011 012 013 014 015 016 017 018 019 020 021 022 023 024 025 026 027 028 029 030 031 032 033 034 035 036 037 038 039 040 041 042 043 044 045 046 047 048 049 050 051 052 053 SEMANTIC ENERGY: DETECTING LLM HALLUCINATION BEYOND ENTROPY

005 **Anonymous authors**

006 Paper under double-blind review

ABSTRACT

011 Large Language Models (LLMs) are being increasingly deployed in real-world
012 applications, but they remain susceptible to hallucinations, which produce fluent
013 yet incorrect responses and lead to erroneous decision-making. Uncertainty
014 estimation is a feasible approach to detect such hallucinations. For example, se-
015 mantic entropy estimates uncertainty by considering the semantic diversity across
016 multiple sampled responses, thus identifying hallucinations. However, seman-
017 tic entropy relies on post-softmax probabilities and fails to capture the model’s
018 inherent uncertainty, causing it to be ineffective in certain scenarios. To ad-
019 dress this issue, we introduce Semantic Energy, a novel uncertainty estimation
020 framework that leverages the inherent confidence of LLMs by operating di-
021 rectly on logits of penultimate layer. By combining semantic clustering with a
022 Boltzmann-inspired energy distribution, our method better captures uncertainty
023 in cases where semantic entropy fails. Experiments across multiple benchmarks
024 show that Semantic Energy significantly improves hallucination detection and un-
025 certainty estimation, offering more reliable signals for downstream applications
026 such as hallucination detection. The code and intermediate data are available at
027 <https://anonymous.4open.science/submit4iclr>.

1 INTRODUCTION

031 Large Language Models (LLMs) have been widely deployed in various aspects of production and
032 daily life, demonstrating strong capabilities in different fields (Schlegel et al., 2025; Xiang et al.,
033 2025). However, LLMs are still prone to being influenced by hallucinations and are prone to gen-
034 erate incorrect answers in situations where they lack knowledge, thus misleading users into making
035 errors (Zhou et al., 2024; Farquhar et al., 2024). Recently, uncertainty estimation has been shown
036 to be a reliable indicator for detecting hallucinations, reflecting the tendency of an LLM to generate
037 hallucinations (Xiao & Wang, 2021; Huang et al., 2024). When the uncertainty of an LLM response
038 is high, it often suggests a greater likelihood that the response is a hallucination, prompting fur-
039 ther actions such as self-reflection (Renze & Guven, 2024; Kirchhof et al., 2025), regenerating of
040 answers (Xu et al., 2025), or intervention by human experts (Liu et al., 2025; Hopkins et al., 2025).

041 Entropy is a commonly used metric for estimating uncertainty in LLM (Cheng et al., 2025; Duan
042 et al., 2024). Similarly to traditional discriminative models, high entropy indicates high uncertainty
043 because it means that the model cannot confidently select a particular outcome. However, due to the
044 nature of natural language, the entropy of a single response cannot accurately reflect the reliability
045 of LLMs. Specifically, even though LLMs may not confidently generate the next token, the semantic
046 meaning of any generated token can still be the same. In such cases, we cannot identify an unreliable
047 response simply attributing to its low probability of being generated. To accurately describe the
048 uncertainty of responses composed of natural language, semantics must be considered.

049 Semantic entropy (Farquhar et al., 2024) is a typical method to characterize the semantic uncer-
050 tainty of responses, effectively representing the probability that an LLM generates hallucinations.
051 Given a question, semantic entropy involves sampling multiple responses, clustering them based
052 on their semantic meaning, and then replacing individual responses with clusters to calculate en-
053 tropy, thus achieving semantic-aware uncertainty characterization. Based on this method, a wide
range of downstream applications have been developed, such as guiding Chain-of-Thought (CoT)
reasoning (Ye et al., 2025) and parallel thinking (Xu et al., 2025). However, semantic entropy has

054 significant drawbacks stemming from entropy itself: it fails to capture the model’s inherent uncer-
 055 tainty, leading to its ineffectiveness in some scenarios.
 056

057 A representative case occurs when the model produces identical responses in multiple sampling
 058 instances for a given question, as illustrated in Fig. 1. According to semantic entropy, the resulting
 059 value is 0, which is considered a reliable response. However, even answering incorrectly, LLMs
 060 might also provide responses with the same semantics. Among samples with consistently semantic
 061 responses across multiple responses, the proportion of incorrect responses (like Question3 in
 062 Fig. 1) approaches 50% in some datasets. In such cases, it is necessary to leverage the model’s
 063 inherent uncertainty for differentiation: even if the LLM provides multiple responses with the same
 064 semantics for two different questions, their corresponding reliability still differs. In scenarios with a
 065 higher inherent uncertainty in the model, the likelihood of the LLM making mistakes is greater.
 066

067 Several previous studies have shown that logits exhibit stronger inherent capabilities to characterize
 068 uncertainty compared to probabilities, and the magnitude of logits can indicate whether the model
 069 has undergone adequate training in a given scenario (Liu et al., 2020; Fu et al., 2025; Zhang et al.,
 070 2024). For example, in out-of-distribution (OOD) detection, studies have highlighted that the logit
 071 values for in-distribution (InD) samples are significantly higher than those for OOD samples (Liu
 072 et al., 2020). Recent work named LogToKU (Ma et al., 2025) points out that probabilities lose the in-
 073 tensity information of logits during normalization, thus limiting their ability to represent the inherent
 074 uncertainty of LLM. From this insight, we propose a new method to improve the failure cases of Se-
 075 mantic Entropy, termed *Semantic Energy*. Specifically, for a given prompt, we first perform multiple
 076 response samplings, followed by semantic sampling. When calculating the final uncertainty, rather
 077 than relying on probability as in Semantic Entropy, we estimate the response uncertainty based on
 078 logits, enabling the estimated uncertainty to reflect the model’s inherent uncertainty. Our proposed
 079 metric significantly outperforms Semantic Entropy in evaluating the reliability of LLM responses,
 080 particularly in scenarios where Semantic Entropy fails. The main contributions are as follows:
 081

- 082 • We expose the limitations of current uncertainty estimation methods based on probability
 083 and identify the failure cases in Semantic Entropy.
- 084 • We introduce **Semantic Energy**, a novel framework to evaluate the uncertainty of LLM
 085 responses, which indicates potential errors in the responses.
- 086 • We instantiate Semantic Energy using the Boltzmann formulation, and in the hallucina-
 087 tion detection task, it achieves an average performance improvement of more than 13%
 088 compared in terms of AUROC to Semantic Entropy in cases where the latter is confident.

089 2 PRELIMINARIES

090 2.1 ESTIMATING LLM UNCERTAINTY WITH TOKEN-LEVEL ENTROPY

091 Let \mathbf{q} denote a natural language query provided as input to the LLM. Given the prompt \mathbf{q} , a single
 092 response sequence is generated in an auto-regressive manner. This response can be represented as:

$$093 \mathbf{x} = [x_1, x_2, \dots, x_T], \quad (1)$$

094 where \mathbf{x} denotes a complete token sequence of variable length T . At each decoding step t , the
 095 model calculates a probability distribution across its entire vocabulary \mathcal{V} , assigning a conditional
 096 probability $p(x_t | x_{<t}, \mathbf{q})$ to each candidate token given the preceding context and the original
 097 query. To quantify the uncertainty in the LLM predictions at each generation step, the token-level
 098 entropy for position t is formally defined as:

$$099 H_t = - \sum_{x \in \mathcal{V}} p(x | x_{<t}, \mathbf{q}) \log p(x | x_{<t}, \mathbf{q}), \quad (2)$$

100 where \mathcal{V} is the model vocabulary. A higher value of H_t indicates a more uniform probability distri-
 101 bution and thus greater uncertainty in the model choice for the t -th token.

102 To estimate the overall uncertainty associated with the entire generated response \mathbf{x} , a common and
 103 straightforward strategy is to aggregate these local token-level entropy values. The most common
 104 aggregation method is to compute the arithmetic mean across all tokens in the sequence:

$$105 H_{\text{avg}}(\mathbf{x}) = \frac{1}{T} \sum_{t=1}^T H_t, \quad (3)$$

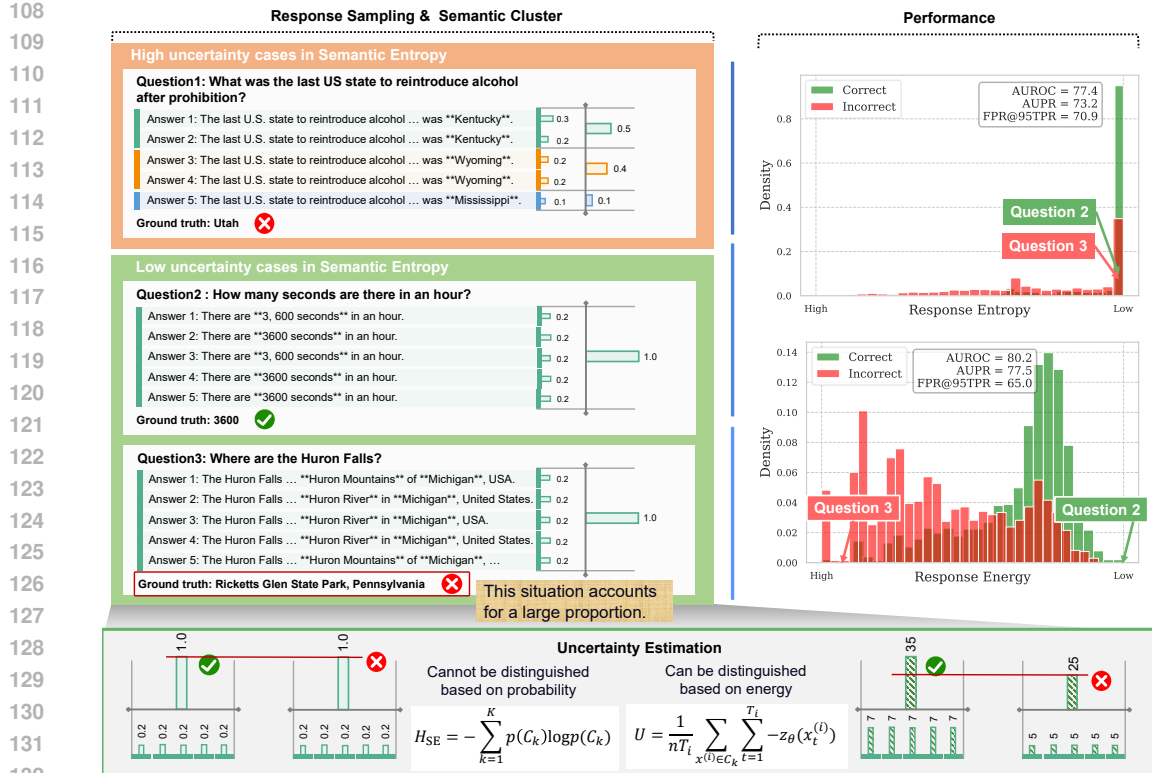


Figure 1: An intuitive comparison between Semantic Entropy and Semantic Energy in their ability to characterize uncertainty. Both approaches first sample and perform semantic clustering over distinct clusters of activity. The difference lies in the computation: Semantic Entropy is calculated based on normalized probabilities, while Semantic Energy is derived from logits. This enables Semantic Energy to distinguish cases when Semantic Entropy fails.

where $H_{avg}(\mathbf{x})$ serves as a proxy for the total uncertainty of the response, with a higher average entropy suggesting a more uncertain generation process. However, this approach implicitly assumes that each token contributes equally to the overall uncertainty, which may not hold in practice.

Recognizing that different tokens can carry varying levels of importance for the meaning and correctness of the final response, some recent studies (Duan et al., 2024) have proposed a refinement employing a weighted average. This method aims to amplify the contribution of critical or pivotal tokens (e.g., those conveying key facts or decisive information) to the final uncertainty score:

$$H_{wavg}(\mathbf{x}) = \sum_{t=1}^T w_t H_t, \quad \text{where } \sum_{t=1}^T w_t = 1, \quad (4)$$

where weights w_t can be determined based on heuristic rules (such as focusing on entities) or learned mechanisms designed to identify semantically important tokens.

Although token-level entropy offers a fine-grained, local perspective on the uncertainty during the auto-regressive generation process, it possesses an inherent limitation: it operates purely on a syntactic or surface level. Quantifies the model's hesitation in choosing the next token, but does not necessarily reflect uncertainty over the underlying meaning or intent of the full response. This is because vastly different token sequences can express the same semantic content, while highly similar token-level probability distributions might lead to responses with divergent meanings. Consequently, token-level metrics may not fully capture the diversity in the semantic content of different possible responses. This critical shortcoming motivates the need for a more holistic, higher-level notion of uncertainty that operates on the distribution of semantically distinct outputs, leading to the concept of *semantic entropy* (Kuhn et al., 2024).

162 2.2 SEMANTIC ENTROPY AND RESPONSE CLUSTERING
163164 To capture semantic-level uncertainty, semantic entropy samples a set of n candidate responses to
165 the query q from LLM:
166

167
$$\mathbb{X} = \{\mathbf{x}^{(1)}, \mathbf{x}^{(2)}, \dots, \mathbf{x}^{(n)}\}, \quad \mathbf{x}^{(i)} = [x_1^{(i)}, x_2^{(i)}, \dots, x_{T_i}^{(i)}], \quad (5)$$

168

169 where $\mathbf{x}^{(i)}$ indicates the i -th sampled response and T_i indicates the number of tokens in this re-
170 sponse. Each response $\mathbf{x}^{(i)}$ has an associated likelihood in the model:
171

172
$$p(\mathbf{x}^{(i)} | \mathbf{q}) = \prod_{t=1}^{T_i} p(x_t^{(i)} | x_{<t}^{(i)}, \mathbf{q}), \quad \bar{p}(\mathbf{x}^{(i)}) = \frac{p(\mathbf{x}^{(i)} | \mathbf{q})}{\sum_{j=1}^n p(\mathbf{x}^{(j)} | \mathbf{q})}. \quad (6)$$

173

174 where $\bar{p}(\mathbf{x}^{(i)})$ indicates a normalized distribution over the sampled responses. Due to surface-level
175 variability in language, semantically similar responses may have different forms. Therefore, semantic
176 entropy clusters the responses into K semantically coherent groups:
177

178
$$\mathbb{C} = \{\mathbb{C}_1, \mathbb{C}_2, \dots, \mathbb{C}_K\}, \quad \mathbb{C}_k \subseteq \mathbb{X}, \quad (7)$$

179

180 where each cluster \mathbb{C}_k contains responses that are semantically equivalent. The probability mass
181 assigned to each cluster is defined as the sum over its members:
182

183
$$p(\mathbb{C}_k) = \sum_{\mathbf{x}^{(i)} \in \mathbb{C}_k} \bar{p}(\mathbf{x}^{(i)}). \quad (8)$$

184

185 Finally, *semantic entropy* (H_{SE}) is computed by applying the standard Shannon entropy formula to
186 this distribution over semantic clusters:
187

188
$$H_{\text{SE}} = - \sum_{k=1}^K p(\mathbb{C}_k) \log p(\mathbb{C}_k), \quad (9)$$

189

190 which quantifies the model’s uncertainty over distinct meanings conveyed by its responses. How-
191 ever, semantic entropy fails in some scenarios due to the limitations of entropy-based uncertainty
192 estimation.
193194 3 MODELING UNCERTAINTY VIA SEMANTIC ENERGY
195196 3.1 LIMITATIONS OF ENTROPY-BASED UNCERTAINTY ESTIMATION
197198 While H_{SE} captures semantic variability, it only reflects *aleatoric uncertainty*—uncertainty arising
199 from intrinsic randomness in the generation process. However, it fails to capture *epistemic uncer-
200 tainty*—uncertainty stemming from the model’s lack of knowledge. For example, as illustrated by
201 the pair of instances in *Low uncertainty cases in Semantic Entropy* (see Fig. 1):
202203

- (1) Consider two queries q_2 and q_3 , where the model has been extensively trained on data
204 related to q_2 (thus confident), but has limited exposure to q_3 (thus uncertain).

205 - (2) Assume that each query is sampled to obtain 5 responses, which were subsequently grouped
206 into a certain cluster based on their semantic similarity ($K = 1$), respectively.

207 - (3) In this case, $H_{\text{SE}} = 0$ for both, despite the LLM outputs 5 incorrect answers on q_3 with the
208 same semantic.

209 This means that if an LLM gives a wrong answer, and the semantics of multiple sampled results
210 are all aligned with that wrong answer, then semantic entropy will mistakenly identify it as reliable.
211 Unfortunately, LLMs are very good at “steadfastly” repeating the same wrong response. In some
212 datasets, nearly half of the samples with repeated identical semantics are actually incorrect answers,
213 making this limitation impossible to ignore.
214215 The reason behind this is that the entropy calculated based on probabilities only reflects the rela-
tive likelihood of a particular LLM response compared to other possible responses generated by the
216

model, rather than the actual probability of that response to the question in the real world. However, when computing the probability of the next token, the model approximates the partition function as the sum of probabilities over its vocabulary. Therefore, for entropy to accurately represent uncertainty, two assumptions must hold: (1) the model has seen all possible responses (that is, the training distribution matches the real-world distribution perfectly), and (2) the model has fit the training distribution without bias (that is, the model output distribution matches the training distribution exactly). Clearly, neither of these assumptions holds. Worse still, the LLM response is based on the joint probability prediction of many tokens, rather than the single word classification of traditional discriminative models, which causes the error of the approximated partition function to accumulate to a degree that can no longer be ignored.

3.2 ENERGY-BASED CONFIDENCE ESTIMATION

To address this limitation, we introduce an energy-based formulation that complements semantic entropy and captures epistemic uncertainty. In thermodynamics of physics, lower energy corresponds to a more stable and less random state. Drawing on thermodynamic analogies, we treat lower-energy states as higher-confidence predictions, following the intuition that physical systems evolve toward minimal-energy configurations.

3.2.1 BOLTZMANN DISTRIBUTION

The classical Boltzmann distribution defines the probability that a system occupying a state is capable of generating $x_t^{(i)}$ as:

$$p(x_t^{(i)}) = \frac{e^{-E_t^{(i)}/k\tau}}{Z_t}, \quad (10)$$

where k is the Boltzmann constant, τ is the temperature, and $E_t^{(i)}$ is the token energy $x_t^{(i)}$, and Z_t is the partition function. Specifically, for LLMs, $Z_t = \sum_{x \in \mathbb{V}} e^{-E_t(x)}$ is the normalization value across the entire vocabulary \mathbb{V} (the difference between \mathcal{V} and \mathbb{V} is that \mathcal{V} is the vocabulary in the predefined tokenizer of a specific LLM, while \mathbb{V} is the space of possible next tokens in the real world, which is infinite and intractable). For simplicity, we assume that Z_t is constant across t . The probability of a complete sequence and the average sequence-level energy can be represented as:

$$p(\mathbf{x}^{(i)}) = \prod_{t=1}^{T_i} p(x_t^{(i)}) = \frac{e^{-\sum_{t=1}^{T_i} E_t^{(i)}}}{\prod_{t=1}^{T_i} Z_t}, \quad E(\mathbf{x}^{(i)}) = \frac{1}{T_i} \sum_{t=1}^{T_i} E_t^{(i)}. \quad (11)$$

Suppose that we want to evaluate the total energy of a set \mathbb{C} . According to the Boltzmann equation, the total energy of \mathbb{C} is the sum of its different states:

$$E_{\text{Bolt}}(\mathbb{C}) = \sum_{\mathbf{x}^{(i)} \in \mathbb{C}} E(\mathbf{x}^{(i)}). \quad (12)$$

Lower energy indicates that the cluster containing this response is more stable, i.e., it has lower uncertainty and thus higher reliability.

3.2.2 SPECIFIC IMPLEMENTATION IN LLMs

For a LLM parameterized by θ with a vocabulary \mathcal{V} , we can formulate the token-level energy distribution within the energy-based modeling framework. Specifically, each token $x_t^{(i)}$ is associated with an energy value $E(x_t^{(i)}, \theta)$, and the probability of generating this token is obtained via a Boltzmann distribution. The partition function Z_θ serves as the normalization term, summing over all possible tokens in the vocabulary \mathcal{V} . This ensures that the resulting distribution is valid and comparable across tokens:

$$p(x_t^{(i)}, \theta) = \frac{e^{-E(x_t^{(i)}, \theta)/k\tau}}{Z_\theta}, \quad Z_\theta = \sum_{x_t^{(i)} \in \mathcal{V}} e^{-E(x_t^{(i)}, \theta)/k\tau}, \quad (13)$$

270 where $k\tau$ corresponds to the temperature parameter that controls the sharpness of the distribution.
 271 The partition function Z_θ reflects the dependence of the probability distribution on the model pa-
 272 rameters θ .

273 From a Bayesian perspective, the total predictive uncertainty of the model should account for uncer-
 274 tainty in the parameters θ themselves. This requires marginalizing over the posterior distribution of
 275 θ given the training data \mathcal{D} . The marginal likelihood of generating a token $x_t^{(i)}$ under this treatment
 276 is expressed as:

$$278 \quad p(x_t^{(i)}, \mathcal{D}) = \int_{\theta} p(x_t^{(i)}, \theta) \cdot p(\theta | \mathcal{D}) d\theta. \quad (14)$$

281 However, we cannot obtain all possible θ , but we can only estimate uncertainty under specific mod-
 282 els. For any given θ , the conditional probability of generating a token from a subset vocabulary
 283 $\mathcal{V} \subseteq \mathbb{V}$ is:

$$284 \quad p(Z_{\theta,t} | Z_t) = \frac{\sum_{x_t^{(i)} \in \mathcal{V}} e^{-E(x_t^{(i)}, \theta)/k\tau}}{\sum_{x_t^{(i)} \in \mathbb{V}} e^{-E(x_t^{(i)}, \theta)/k\tau}}. \quad (15)$$

287 By combining this subset-based probability with Eq. 14, we can approximate the marginal distribu-
 288 tion using the current model parameters. The resulting sampled approximation is given by:

$$290 \quad \tilde{p}(x_t^{(i)}, \mathcal{D}) = p(x_t^{(i)}, \theta) \cdot p(Z_{\theta,t} | Z_t) = \frac{e^{-E(x_t^{(i)}, \theta)/k\tau}}{Z_t}, \quad (16)$$

292 where $\tilde{p}(x_t^{(i)}, \mathcal{D})$ indicates a sampled approximation of $p(x_t^{(i)}, \mathcal{D})$. Similarly to softmax-based prob-
 293 ability modeling, the probability of a complete sequence is the joint probability of all tokens in the
 294 entire sequence:

$$295 \quad \tilde{p}(\mathbf{x}^{(i)}) = \prod_{t=1}^{T_i} \tilde{p}(x_t^{(i)}) = \frac{e^{-\sum_{t=1}^{T_i} \tilde{E}_t^{(i)}/k\tau}}{\prod_{t=1}^{T_i} Z_t}, \quad \tilde{E}(\mathbf{x}^{(i)}) = \frac{1}{T_i} \sum_{t=1}^{T_i} \tilde{E}_t^{(i)}, \quad (17)$$

298 where $\tilde{E}(\mathbf{x}^{(i)})$ indicates the average sequence-level energy, which can also be interpreted as the
 299 energy per unit volume in thermodynamics, that is, the free energy density (Callen, 1993). To
 300 extend to semantic clusters, we treat each cluster \mathbb{C}_k energy as a scaled joint energy:

$$301 \quad \tilde{E}_{\text{Bolt}}(\mathbb{C}_k) = \frac{1}{n} \sum_{\mathbf{x}^{(i)} \in \mathbb{C}_k} \tilde{E}(\mathbf{x}^{(i)}), \quad (18)$$

303 where n are the sampling times for every question.

305 For an LLM trained with cross-entropy loss, we represent $E(x_t^{(i)}, \theta)$ as the negative value of the
 306 logit, that is, $E(x_t^{(i)}, \theta) = -z_\theta(x_t^{(i)})$, and $k\tau$ is by default the temperature used during LLM train-
 307 ing, that is, $k\tau = 1$. The final uncertainty is defined as:

$$309 \quad U(\mathbf{x}^{(i)}) = \frac{1}{n} \sum_{\mathbf{x}^{(j)} \in \mathbb{C}_k} \frac{1}{T_j} \sum_{t=1}^{T_j} -z_\theta(x_t^{(j)}), \quad \forall \mathbf{x}^{(i)} \in \mathbb{C}_k, \quad (19)$$

311 which captures the average negative logit across tokens and samples. The lower energy corresponds
 312 to the lower uncertainty, thus establishing a direct connection between model confidence and energy-
 313 based representation. The uncertainty of a single reply is represented by the uncertainty of the
 314 semantic cluster to which it belongs. That is, for all replies that belong to the same semantic cluster,
 315 their uncertainty is identical.

317 4 EXPERIMENTS

319 4.1 SETUP

321 **Model & Baseline.** We conduct experiments using the Qwen3-8B model (Yang et al., 2025), and
 322 the ERNIE-21B-A3B model (MOE architecture) (Baidu, 2025). Our primary goal is to highlight the
 323 differences between probability-based methods and energy-based approaches. Therefore, we use
 the semantic entropy (Farquhar et al., 2024) as a baseline.

Datasets & Metrics. Experiments are performed on standard open-domain QA datasets in both Chinese and English: the Chinese dataset *CSQA* (He et al., 2024) and the English dataset *TriviaQA* (Joshi et al., 2017). To assess whether the estimated uncertainty can capture the risk that the model makes errors, we estimate the AUROC between uncertainty scores and correctness (i.e., whether the answer is correct).

4.2 MAIN RESULTS

Table 1: Uncertainty estimation performance on OpenQA Datasets.

Model	Dataset	Semantic Entropy			Semantic Energy		
		AUROC	AUPR	FPR95	AUROC _(↑)	AUPR _(↑)	FPR95 _(↓)
Qwen3-8B	CSQA	71.6%	53.6%	77.0%	76.1% \uparrow 4.5%	61.4% \uparrow 7.8%	74.6% \uparrow 2.4%
	TriviaQA	69.6%	73.5%	79.1%	74.8% \uparrow 5.2%	79.2% \uparrow 5.7%	74.7% \uparrow 4.4%
ERNIE-21B-A3B	CSQA	77.4%	73.2%	70.9%	80.2% \uparrow 2.8%	77.5% \uparrow 4.3%	65.0% \uparrow 5.9%
	TriviaQA	75.1%	85.0%	69.9%	81.0% \uparrow 5.9%	89.9% \uparrow 4.9%	63.7% \uparrow 6.2%

Table 1 summarizes the performance of uncertainty estimation methods on the CSQA and TriviaQA datasets. We evaluate models using standard metrics: AUROC, AUPR, and FPR@95, based on whether the uncertainty score can discriminate correct from incorrect responses.

In both models and datasets, *semantic energy* consistently outperforms *semantic entropy*. On CSQA, the Boltzmann energy improves AUROC from 71.6% to 76.1% on Qwen3-8B and from 77.4% to 80.2% on ERNIE-21B-A3B. Similar trends are observed on TriviaQA, where Boltzmann energy yields AUROC gains of more than 5% compared to the semantic entropy. Improvements are also reflected in AUPR and FPR@95, indicating better calibration and reduced false positive rates.

These results highlight the robustness of energy-based uncertainty estimation, particularly in low-diversity scenarios where entropy becomes degenerate (details in Table 2). By incorporating internal model states via logits, semantic energy captures a richer signal for uncertainty estimation beyond probability-based entropy.

4.3 ABLATION STUDIES

4.3.1 RESULTS ON QUESTIONS WITH SINGLE CLUSTER

Table 2: Uncertainty estimation performance on questions with **single** cluster.

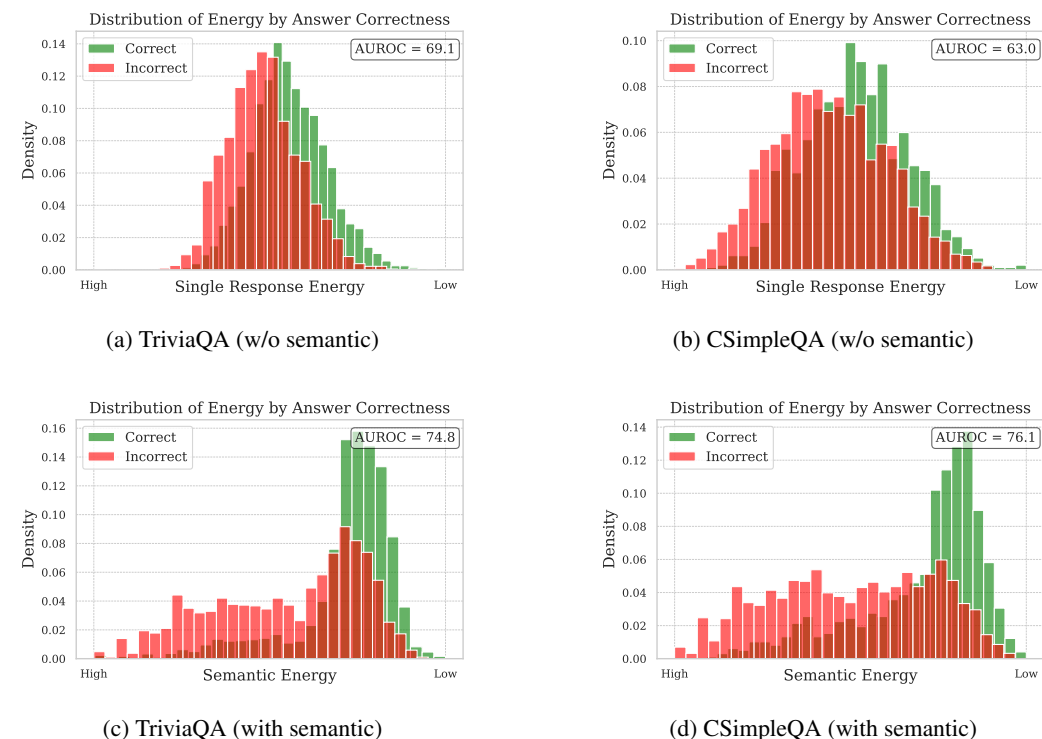
Model	Dataset	Semantic Entropy			Semantic Energy		
		AUROC	AUPR	FPR95	AUROC _(↑)	AUPR _(↑)	FPR95 _(↓)
Qwen3-8B	CSQA	50.0%	55.8%	95.0%	66.7% \uparrow 16.7%	67.6% \uparrow 11.8%	80.3% \uparrow 14.7%
	TriviaQA	50.0%	75.1%	95.0%	62.1% \uparrow 12.1%	81.6% \uparrow 6.5%	86.9% \uparrow 8.1%
ERNIE-21B-A3B	CSQA	50.0%	77.0%	95.0%	58.9% \uparrow 8.9%	81.9% \uparrow 4.9%	88.4% \uparrow 6.6%
	TriviaQA	50.0%	85.9%	95.0%	65.8% \uparrow 15.8%	91.4% \uparrow 5.5%	83.4% \uparrow 11.6%

In Table 2, we present the case where all responses share the same semantics, that is, all responses are clustered into a single group as described in Sec. 3.1. In this scenario, semantic entropy completely fails, whereas semantic energy is still able to provide a certain level of distinction, resulting in semantic energy achieving an average performance improvement of more than 13% compared in terms of AUROC to semantic entropy in cases where the latter is confident. It is important to note that the value of semantic entropy in such cases is always zero, meaning that its performance reflects the expected performance when the uncertainty indicator is meaningless, for example, the AUPR corresponds to the number of positive samples (i.e. correct responses).

4.3.2 ADVANTAGES OF SEMANTIC CLUSTER

Inspired by semantic entropy, we incorporate semantic influence when computing energy. If semantics are not considered and the energy of a single response is directly used to characterize the

378 reliability of an LLM’s reply, such as in LogTokU (Ma et al., 2025), a clear problem arises: a single
 379 response having high energy does not necessarily mean that the entire cluster of responses sharing
 380 the same semantics also has high energy. This is because different responses belonging to the same
 381 semantic cluster can still have varying energy values. Therefore, we represent the energy of a re-
 382 sponse by the energy of the cluster to which it belongs. As shown in Fig. 2, we conduct an ablation
 383 study on whether to include semantics. The experimental results demonstrate that incorporating
 384 semantics significantly improves the accuracy of uncertainty estimation.



410 Figure 2: Comparison of semantic vs. non-semantic uncertainty modeling on TriviaQA and CSim-
 411 pleQA datasets.

413 4.3.3 RESULTS ON THINK MODE

415 To validate the performance of the proposed method on the thinking model, we conduct experiments
 416 on Qwen-8B using the CSQA dataset and explore the case where the think mode is enabled. Specif-
 417 ically, we activate the think mode but discard the content within `<think>...<think>` during
 418 evaluation, considering only the response portion. The final results, shown in Fig. 3, are consistent
 419 with the observations in Table 1. This indicates that even when the LLM undergoes a lengthy think-
 420 ing process during output generation, its final results can still accurately capture the uncertainty of
 421 the model’s responses through logits, thereby reflecting the reliability of the answers. Additionally,
 422 we observe that both semantic entropy and semantic energy demonstrate significantly improved un-
 423 certainty characterization capabilities in the think mode compared to the performance reported in
 424 Table 1. This suggests that the context during the deep thinking process may positively contribute
 425 to characterizing the distributional uncertainty of the final responses.

426 5 RELATED WORK

427 **Uncertainty estimation methods.** Recently, numerous uncertainty estimation methods for LLMs
 428 have been proposed. These include methods that utilize natural language for uncertainty feedback,
 429 including heuristically designed and trained approaches (Tao et al., 2025; Xiong et al., 2023; Lin
 430 et al., 2023); methods that estimate uncertainty based on model states, including those leveraging

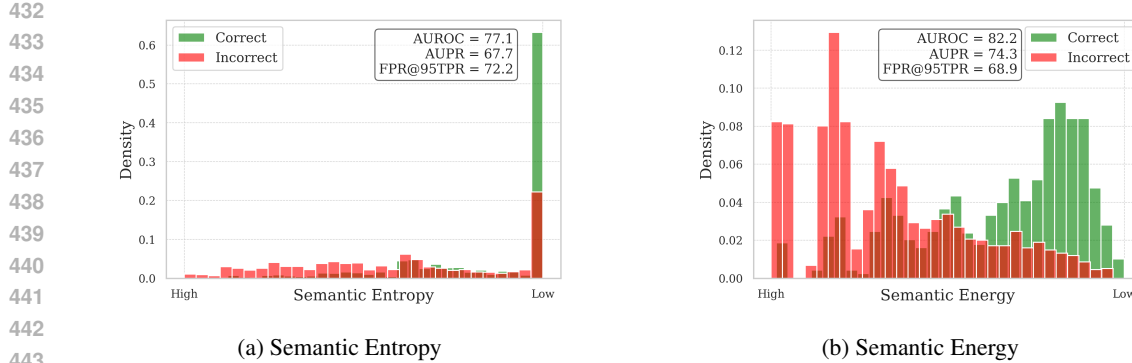


Figure 3: Comparison of semantic entropy vs. semantic energy on CSQA datasets with think mode on.

prior knowledge or statistical observations of model states (Kostenok et al., 2023; Li et al., 2025; Liu et al., 2024), or observing changes under perturbations (Zhang et al., 2025b; Gao et al., 2024); and methods that take into account the semantics of the response, including consistency-based uncertainty characterizations (Lyu et al., 2025; Bartsch et al., 2023; Xiao et al., 2025) and approaches that integrate semantics with model states (Kuhn et al., 2024; Grewal et al., 2024).

Uncertainty-guided applications. The utilization of uncertainty estimation is widely applied in both the post-train and inference phases of LLMs. For example, minimizing entropy during the reinforcement learning process helps reduce uncertainty (Zhang et al., 2025a; Agarwal et al., 2025) and encourages exploration of critical positions with higher uncertainty (Zheng et al., 2025; Cheng et al., 2025). In the inference phase, uncertainty has emerged as a powerful signal for guiding LLMs and related systems. For example, Ye et al. (2025) introduce CoT Entropy to quantify the uncertainty of a PRM in stepwise verification, while Wang et al. (2022) demonstrate that monitoring uncertainty across multiple reasoning paths helps select more reliable outputs. In retrieval-augmented generation (RAG), Guo et al. (2025) propose empowering retrieval decisions with model confidence, and Chen & Varoquaux (2025) provide *internal confidence* to improve RAG on factual QA and mathematical reasoning tasks. In multi-agent and collaborative systems, Dey et al. (2025) propose *uncertainty-aware fusion* to reduce hallucinations by strategically combining multiple LLM based on their accuracy and self-assessment abilities. Kruse et al. (2025) propose *multi-LLM uncertainty via subset ensembles* that uses Jensen-Shannon Divergence to identify and aggregate well-calibrated subsets of LLMs. Uncertainty can also be used to determine when to stop or skip reasoning. Xu et al. (2025) design adaptive stopping criteria where the model halts reasoning once confidence exceeds a threshold, reducing unnecessary computation, and Zhu et al. (2025) propose *UnCert-CoT* that uncertainty-aware skipping prevents overthinking by allowing the model to bypass low-value reasoning steps.

6 DISCUSSION AND CONCLUSION

In this paper, we introduce the concept of semantic energy as an enhancement of semantic entropy, an uncertainty modeling method that substitutes entropy with energy (derived from logits). Semantic energy can effectively compensate for the shortcomings of semantic entropy and better capture the inherent uncertainty within models. We also clarify the limitations imposed by probability normalization and demonstrate the potential to overcome these constraints. Although logits are not strictly equivalent to energy, they exhibit energy-like characteristics solely due to the implicit constraints arising from network initialization and regularization during training. This property of logits has been leveraged in many previous studies, such as in the field of OOD detection. Furthermore, future LLM development should consider the limitations associated with probability-based training to mitigate performance degradation caused by factors such as training data distribution.

486 REFERENCES
487

488 Shivam Agarwal, Zimin Zhang, Lifan Yuan, Jiawei Han, and Hao Peng. The unreasonable effec-
489 tiveness of entropy minimization in llm reasoning. *arXiv preprint arXiv:2505.15134*, 2025.

490 Baidu. Ernie 4.5 technical report. Technical report, Baidu, 2025. URL https://yiyan.baidu.com/blog/publication/ERNIE_Technical_Report.pdf. Accessed: 2025-07-30.

491

492 Henning Bartsch, Ole Jorgensen, Domenic Rosati, Jason Hoelscher-Obermaier, and Jacob Pfau.
493 Self-consistency of large language models under ambiguity. *arXiv preprint arXiv:2310.13439*,
494 2023.

495

496 Herbert B Callen. Thermodynamics and an introduction to thermostatistics. *John Wiley & Sons*, 2,
497 1993.

498

499 Lihu Chen and Gaël Varoquaux. Query-level uncertainty in large language models. *arXiv preprint*
500 *arXiv:2506.09669*, 2025.

501

502 Daixuan Cheng, Shaohan Huang, Xuekai Zhu, Bo Dai, Wayne Xin Zhao, Zhenliang Zhang, and
503 Furu Wei. Reasoning with exploration: An entropy perspective. *arXiv preprint arXiv:2506.14758*,
504 2025.

505

506 Prasenjit Dey, Srujan Merugu, and Sivaramakrishnan Kaveri. Uncertainty-aware fusion: An ensem-
507 ble framework for mitigating hallucinations in large language models. In *Companion Proceedings*
508 of the ACM on Web Conference 2025, pp. 947–951, 2025.

509

510 Jinhao Duan, Hao Cheng, Shiqi Wang, Alex Zavalny, Chenan Wang, Renjing Xu, Bhavya Kailkhura,
511 and Kaidi Xu. Shifting attention to relevance: Towards the predictive uncertainty quantification of
512 free-form large language models. In *Proceedings of the 62nd Annual Meeting of the Association*
513 for *Computational Linguistics (Volume 1: Long Papers)*, pp. 5050–5063, 2024.

514

515 Sebastian Farquhar, Jannik Kossen, Lorenz Kuhn, and Yarin Gal. Detecting hallucinations in large
516 language models using semantic entropy. *Nature*, 630(8017):625–630, 2024.

517

518 Tianyu Fu, Yi Ge, Yichen You, Enshu Liu, Zhihang Yuan, Guohao Dai, Shengen Yan, Huazhong
519 Yang, and Yu Wang. R2r: Efficiently navigating divergent reasoning paths with small-large model
520 token routing. *arXiv preprint arXiv:2505.21600*, 2025.

521

522 Xiang Gao, Jiaxin Zhang, Lalla Mouatadid, and Kamalika Das. Spuq: Perturbation-based uncer-
523 tainty quantification for large language models. *arXiv preprint arXiv:2403.02509*, 2024.

524

525 Yashvir S Grewal, Edwin V Bonilla, and Thang D Bui. Improving uncertainty quantification in large
526 language models via semantic embeddings. *arXiv preprint arXiv:2410.22685*, 2024.

527

528 Kai Guo, Harry Shomer, Shenglai Zeng, Haoyu Han, Yu Wang, and Jiliang Tang. Empowering
529 graphrag with knowledge filtering and integration. *arXiv preprint arXiv:2503.13804*, 2025.

530

531 Yancheng He, Shilong Li, Jiaheng Liu, Yingshui Tan, Weixun Wang, Hui Huang, Xingyuan Bu,
532 Hangyu Guo, Chengwei Hu, Boren Zheng, et al. Chinese simpleqa: A chinese factuality evalua-
533 tion for large language models. *arXiv preprint arXiv:2411.07140*, 2024.

534

535 Aspen Hopkins, Angie Boggust, and Harini Suresh. Chatbot evaluation is (sometimes) ill-posed:
536 Contextualization errors in the human-interface-model pipeline. 2025.

537

538 Hsiu-Yuan Huang, Yutong Yang, Zhaoxi Zhang, Sanwoo Lee, and Yunfang Wu. A survey of uncer-
539 tainty estimation in llms: Theory meets practice. *arXiv preprint arXiv:2410.15326*, 2024.

540

541 Mandar Joshi, Eunsol Choi, Daniel S Weld, and Luke Zettlemoyer. Triviaqa: A large scale distantly
542 supervised challenge dataset for reading comprehension. *arXiv preprint arXiv:1705.03551*, 2017.

543

544 Michael Kirchhof, Luca Füger, Adam Goliński, Eeshan Gunesh Dhekane, Arno Blaas, and Sinead
545 Williamson. Self-reflective uncertainties: Do llms know their internal answer distribution? *arXiv*
546 *preprint arXiv:2505.20295*, 2025.

540 Elizaveta Kostenok, Daniil Cherniavskii, and Alexey Zaytsev. Uncertainty estimation of trans-
 541 formers’ predictions via topological analysis of the attention matrices. *arXiv preprint*
 542 *arXiv:2308.11295*, 2023.

543

544 Maya Kruse, Majid Afshar, Saksham Khatwani, Anoop Mayampurath, Guanhua Chen, and Yanjun
 545 Gao. An information-theoretic perspective on multi-llm uncertainty estimation. *medRxiv*, pp.
 546 2025–07, 2025.

547

548 Lorenz Kuhn, Yarin Gal, and Sebastian Farquhar. Semantic uncertainty: Linguistic invariances for
 549 uncertainty estimation in natural language generation. *Nature*, 2024.

550

551 Yinghao Li, Rushi Qiang, Lama Moukheiber, and Chao Zhang. Language model uncertainty quan-
 552 tification with attention chain. *arXiv preprint arXiv:2503.19168*, 2025.

553

554 Zhen Lin, Shubhendu Trivedi, and Jimeng Sun. Generating with confidence: Uncertainty quantifi-
 555 cation for black-box large language models. *arXiv preprint arXiv:2305.19187*, 2023.

556

557 Jingyu Liu, Jingquan Peng, Xubin Li, Tiezheng Ge, Bo Zheng, Yong Liu, et al. Do not abstain!
 558 identify and solve the uncertainty. *arXiv preprint arXiv:2506.00780*, 2025.

559

560 Linyu Liu, Yu Pan, Xiaocheng Li, and Guanting Chen. Uncertainty estimation and quantification
 561 for llms: A simple supervised approach, 2024. URL <https://arxiv.org/abs/2404.15993>, 2024.

562

563 Weitang Liu, Xiaoyun Wang, John Owens, and Yixuan Li. Energy-based out-of-distribution detec-
 564 tion. *Advances in neural information processing systems*, 33:21464–21475, 2020.

565

566 Qing Lyu, Kumar Shridhar, Chaitanya Malaviya, Li Zhang, Yanai Elazar, Niket Tandon, Marianna
 567 Apidianaki, Mrinmaya Sachan, and Chris Callison-Burch. Calibrating large language models with
 568 sample consistency. In *Proceedings of the AAAI Conference on Artificial Intelligence*, volume 39,
 569 pp. 19260–19268, 2025.

570

571 Huan Ma, Jingdong Chen, Joey Tianyi Zhou, Guangyu Wang, and Changqing Zhang. Estimating
 572 llm uncertainty with evidence. *arXiv preprint arXiv:2502.00290*, 2025.

573

574 Matthew Renze and Erhan Guven. Self-reflection in llm agents: Effects on problem-solving perfor-
 575 mance. *arXiv preprint arXiv:2405.06682*, 2024.

576

577 Katja Schlegel, Nils R Sommer, and Marcello Mortillaro. Large language models are proficient in
 578 solving and creating emotional intelligence tests. *Communications Psychology*, 3(1):80, 2025.

579

580 Linwei Tao, Yi-Fan Yeh, Minjing Dong, Tao Huang, Philip Torr, and Chang Xu. Revisiting un-
 581 certainty estimation and calibration of large language models. *arXiv preprint arXiv:2505.23854*,
 582 2025.

583

584 Xuezhi Wang, Jason Wei, Dale Schuurmans, Quoc Le, Ed Chi, Sharan Narang, Aakanksha Chowdh-
 585 ery, and Denny Zhou. Self-consistency improves chain of thought reasoning in language models.
 586 *arXiv preprint arXiv:2203.11171*, 2022.

587

588 Jinxi Xiang, Xiyue Wang, Xiaoming Zhang, Yinghua Xi, Feyisope Eweje, Yijiang Chen, Yuchen
 589 Li, Colin Bergstrom, Matthew Gopaulchan, Ted Kim, et al. A vision–language foundation model
 590 for precision oncology. *Nature*, 638(8051):769–778, 2025.

591

592 Quan Xiao, Debarun Bhattacharjya, Balaji Ganeshan, Radu Marinescu, Katsiaryna Mirylenka,
 593 Nhan H Pham, Michael Glass, and Junkyu Lee. The consistency hypothesis in uncertainty quan-
 594 tification for large language models. *arXiv preprint arXiv:2506.21849*, 2025.

595

596 Yijun Xiao and William Yang Wang. On hallucination and predictive uncertainty in conditional
 597 language generation, 2021. URL <https://arxiv.org/abs/2103.15025>.

598

599 Miao Xiong, Zhiyuan Hu, Xinyang Lu, Yifei Li, Jie Fu, Junxian He, and Bryan Hooi. Can llms
 600 express their uncertainty? an empirical evaluation of confidence elicitation in llms. *arXiv preprint*
 601 *arXiv:2306.13063*, 2023.

594 Zenan Xu, Zexuan Qiu, Guanhua Huang, Kun Li, Siheng Li, Chenchen Zhang, Kejiao Li, Qi Yi,
 595 Yuhao Jiang, Bo Zhou, et al. Adaptive termination for multi-round parallel reasoning: An univer-
 596 sal semantic entropy-guided framework. *arXiv preprint arXiv:2507.06829*, 2025.

597
 598 An Yang, Anfeng Li, Baosong Yang, Beichen Zhang, Binyuan Hui, Bo Zheng, Bowen Yu,
 599 Chang Gao, Chengen Huang, Chenxu Lv, et al. Qwen3 technical report. *arXiv preprint*
 600 *arXiv:2505.09388*, 2025.

601
 602 Zihuiwen Ye, Luckeciano Carvalho Melo, Younesse Kaddar, Phil Blunsom, Sam Staton, and Yarin
 603 Gal. Uncertainty-aware step-wise verification with generative reward models. *arXiv preprint*
 604 *arXiv:2502.11250*, 2025.

605
 606 Jianyi Zhang, Da-Cheng Juan, Cyrus Rashtchian, Chun-Sung Ferng, Heinrich Jiang, and Yiran
 607 Chen. Sled: Self logits evolution decoding for improving factuality in large language models.
 608 *Advances in Neural Information Processing Systems*, 37:5188–5209, 2024.

609
 610 Qingyang Zhang, Haitao Wu, Changqing Zhang, Peilin Zhao, and Yatao Bian. Right question
 611 is already half the answer: Fully unsupervised llm reasoning incentivization. *arXiv preprint*
 612 *arXiv:2504.05812*, 2025a.

613
 614 Tunyu Zhang, Haizhou Shi, Yibin Wang, Hengyi Wang, Xiaoxiao He, Zhuowei Li, Haoxian Chen,
 615 Ligong Han, Kai Xu, Huan Zhang, et al. Token-level uncertainty estimation for large language
 616 model reasoning. *arXiv preprint arXiv:2505.11737*, 2025b.

617
 618 Tianyu Zheng, Tianshun Xing, Qingshui Gu, Taoran Liang, Xingwei Qu, Xin Zhou, Yizhi Li, Zhou-
 619 futu Wen, Chenghua Lin, Wenhao Huang, et al. First return, entropy-eliciting explore. *arXiv*
 620 *preprint arXiv:2507.07017*, 2025.

621
 622 Lexin Zhou, Wout Schellaert, Fernando Martínez-Plumed, Yael Moros-Daval, Cèsar Ferri, and José
 623 Hernández-Orallo. Larger and more instructable language models become less reliable. *Nature*,
 624 634(8032):61–68, 2024.

625
 626 Yuqi Zhu, Ge Li, Xue Jiang, Jia Li, Hong Mei, Zhi Jin, and Yihong Dong. Uncertainty-guided
 627 chain-of-thought for code generation with llms. *arXiv preprint arXiv:2503.15341*, 2025.

648 A PROMPTS FOR DIFFERENT EXPERIMENTS
649650 Prompt for Response Sampling
651652 According to official recommendations, we adopted the following prompts for Qwen3
653 and ERNIE respectively.
654655 **Qwen-3 Prompt:**
656 <|im_start|>user\n {question} Give a short answer:
657 <|im_end|>\n <|im_start|>assistant\n658 **ERNIE-4.5 Prompt:**
659 <|begin_of_sentence|>User: {question} Give a short answer:\n
660 Assistant:
661662 Prompt for Semantic Cluster
663664 We utilize the **TIGER-Lab/general-verifier** model for semantic clustering,
665 which analyzes whether different answers convey the same meaning for a given ques-
666 tion.
667668 <|im_start|>system Please reason step by step, and put your
669 final answer within \boxed{ }. <|im_end|>\n <|im_start|>user\n
670 {question} \n\n{answer_a} \n\n{answer_b} \n\nFor the above
671 question, please verify if the student's answer is equivalent
672 to the ground truth answer.\nDo not solve the question by
673 yourself; just check if the student's answer is equivalent to
674 the ground truth answer.\nIf the student's answer is correct,
675 output "Final Decision: Yes". If the student's answer
676 is incorrect, output "Final Decision: No". Assistant:
677 <|im_end|>\n <|im_start|>assistant678
679 Prompt for Judgment
680681 During the judgement process, **TIGER-Lab/general-verifier** is employed to de-
682 termine whether the model's response aligns with the ground truth answer.
683684 <|im_start|>system Please reason step by step, and put your
685 final answer within \boxed{ }. <|im_end|>\n <|im_start|>user\n
686 {question} \n\n{l1m_response} \n\n{ground_truth} \n\nFor the above
687 question, please verify if the student's answer is equivalent
688 to the ground truth answer.\nDo not solve the question by
689 yourself; just check if the student's answer is equivalent to
690 the ground truth answer.\nIf the student's answer is correct,
691 output "Final Decision: Yes". If the student's answer
692 is incorrect, output "Final Decision: No". Assistant:
693 <|im_end|>\n <|im_start|>assistant694
695 B DETAILS FOR COMPARISON METHODS
696697 In this paper, we primarily compare our method with the well-known approach, semantic entropy.
698 Since both methods require response sampling and semantic clustering, we use identical data for
699 these parts. That is, the only difference lies in the final uncertainty calculation process, in which
700 the responses and clusters are generated from the same set of data. For the TriviaQA dataset, due to
701 its large number of entries, we only estimate results for the first 5,000 samples. Note that this is a
commonly adopted practice. Additionally, the sampling temperature is set to 0.6, as recommended

702 in the official documentation, and the random seed is set to values from 1 to 10 to sample ten distinct
 703 responses.
 704

705 It is important to note that the value of semantic entropy in table 2 is always zero, meaning that its
 706 performance reflects the **expected** result when the uncertainty indicator is meaningless; for example,
 707 the AUPR corresponds to the number of positive samples (i.e. correct responses).

708
 709 **C PSEUDO CODE**
 710

711 **Algorithm 1: Semantic Energy-based Uncertainty Estimation**
 712

713 **Input:** Natural language query \mathbf{q} , LLM with parameters θ , sampling times n
 714 **Output:** Semantic clusters $\mathbb{C} = \{\mathbb{C}_1, \dots, \mathbb{C}_K\}$ and their uncertainties $U(\mathbb{C}_k)$

715 **1 Step 1: Response Sampling**

716 **2 for** $i = 1$ **to** n **do**

717 **3 Sample response** $\mathbf{x}^{(i)} = [x_1^{(i)}, \dots, x_{T_i}^{(i)}]$ **from LLM;**

718 **4 for** $t = 1$ **to** T_i **do**

719 **5 Record logit** $z_\theta(x_t^{(i)})$;

720 **6 Record probability** $p(x_t^{(i)} | x_{<t}^{(i)}, \mathbf{q})$;

721 **7 end**

722 **8 end**

723 **9 Step 2: Semantic Clustering**

724 **10 Initialize** $\mathbb{C} \leftarrow \emptyset$;

725 **11 foreach** pair $(\mathbf{x}^{(i)}, \mathbf{x}^{(j)})$ **do**

726 **12 Use semantic verifier to test equivalence;**

727 **13 if** equivalent **then**

728 **14 Assign** $\mathbf{x}^{(i)}, \mathbf{x}^{(j)}$ **to the same cluster;**

729 **15 end**

730 **16 end**

731 **17 Obtain** $\mathbb{C} = \{\mathbb{C}_1, \dots, \mathbb{C}_K\}$;

732 **18 Step 3: Energy-Based Reliability**

733 **19 foreach** response $\mathbf{x}^{(i)}$ **do**

734 **20 Compute average energy:**

$$\tilde{E}(\mathbf{x}^{(i)}) = \frac{1}{T_i} \sum_{t=1}^{T_i} -z_\theta(x_t^{(i)})$$

735 **21 end**

736 **22 foreach** cluster \mathbb{C}_k **do**

737 **23 Compute cluster uncertainty:**

$$U(\mathbb{C}_k) = \frac{1}{|\mathbb{C}_k|} \sum_{\mathbf{x}^{(i)} \in \mathbb{C}_k} \tilde{E}(\mathbf{x}^{(i)})$$

738 **24 end**

739 **25 foreach** response $\mathbf{x}^{(i)} \in \mathbb{C}_k$ **do**

740 **26 Assign uncertainty** $U(\mathbf{x}^{(i)}) = U(\mathbb{C}_k)$;

741 **27 end**

742

743

744

745

746

747

748

749

750

751

752 **D THE USE OF LLMs**
 753

754 After completing the paper, we used an LLM to check for grammatical errors in the text, thereby
 755 ensuring that the paper was free of writing issues. At the same time, we continuously submitted
 updated versions to different LLMs, such as ChatGPT, for simulated review, which helped supple-

756
 757
 758
 759
 760
 761
 762
 763
 764
 765
 766
 767
 768
 769
 770
 771
 772
 773
 774
 775
 776
 777
 778
 779
 780
 781
 782
 783
 784
 785
 786
 787
 788
 789
 790
 791
 792
 793
 794
 795
 796
 797
 798
 799
 800
 801
 802
 803
 804
 805
 806
 807
 808
 809
 810

ment additional experiments and related work analyses. It is worth noting that although our final version satisfied the LLMs, our goal was not to make the LLMs happy with the revisions. Instead, we engaged in additional discussions and made modifications based on the potential shortcomings pointed out by the LLMs, continually refining the paper into its final form. While ensuring it meets the approval of peers, we also made sure the LLM considered this paper an outstanding piece of work.

E ATTEMPTS ON THE FERMI-DIRAC DISTRIBUTION

E.1 FERMI-DIRAC DISTRIBUTION

To account for potential dependencies among samples, we generalize to the expected energy:

$$E(\mathbb{C}_k) = \sum_{\mathbf{x}^{(i)} \in \mathbb{C}_k} p(\mathbf{x}^{(i)}) E(\mathbf{x}^{(i)}). \quad (20)$$

Since exact Z is intractable in Boltzmann distribution, we also consider the **Fermi–Dirac distribution**:

$$p(\mathbf{x}^{(i)}) = \frac{1}{e^{(E(\mathbf{x}^{(i)}) - \mu)/kT} + 1}, \quad (21)$$

where μ (chemical potential) is approximated as the mean of all logits across tokens and samples. This form reflects saturation effects and confidence plateauing.

The corresponding energy is defined as:

$$E_{\text{Fermi}}(\mathbb{C}_k) = \sum_{\mathbf{x}^{(i)} \in \mathbb{C}_k} \frac{E(\mathbf{x}^{(i)})}{e^{(E(\mathbf{x}^{(i)}) - \mu)/kT} + 1}. \quad (22)$$

E.2 HYPER-PARAMETERS IN FERMI-DIRAC DISTRIBUTION

In the Fermi–Dirac-based uncertainty formulation, the chemical potential μ plays a critical role in shaping the distribution and consequently in estimating model confidence. To investigate its effect, we empirically examined how the quality of uncertainty estimation varies with different choices of μ . When μ is initially set to match the Boltzmann distribution regime (that is, very negative values), the Fermi–Dirac model behaves similarly to the exponential Boltzmann case. As μ increases, the performance first improves and reaches a peak, after which it drops rapidly, indicating a sharp sensitivity to this parameter.

From a physical perspective, the chemical potential μ in the Fermi–Dirac distribution determines the energy level at which the probability of occupation is 1/2. In our setup, we interpret μ as a learned threshold separating high-confidence and low-confidence generations. To avoid manual tuning and leverage the thermodynamic grounding of the method, we solve for the optimal μ analytically by enforcing the self-consistency condition.

$$\frac{1}{n} \sum_{i=1}^n \frac{1}{e^{(E(\mathbf{x}^{(i)}) - \mu)/kT} + 1} = \mu, \quad (23)$$

which is derived from the condition that the mean value of the Fermi–Dirac occupation function is equal to μ itself. This fixed-point equation,

$$\mathbb{E}_{\mathbf{x} \sim \mathbb{X}} \left[\frac{1}{e^{(E(\mathbf{x}) - \mu)/kT} + 1} \right] = \mu,$$

yields the *system-consistent* value of μ , ensuring that the modeled uncertainty distribution reflects a stable equilibrium in the energy landscape. Numerically, we solve Eq. 23 using root-finding methods (e.g., bisection or Newton-Raphson), producing an interpretable and data-adaptive setting of μ without requiring heuristic tuning. However, these observations are not consistently manifested in all models and require further exploration.